Carbohydrate Polymers 112 (2014) 422–431

Contents lists available at ScienceDirect

Carbohydrate Polymers

journal homepage: www.elsevier.com/locate/carbpol

Correlation of chemical, structural and thermal properties of natural fibres for their sustainable exploitation

Rosana Moriana[a,b,*], Francisco Vilaplana[a,c,d], Sigbritt Karlsson[a,e], Amparo Ribes[b]

[a] School of Chemical Science and Engineering, Fibre and Polymer Technology, Royal Institute of Technology, Teknikringen 56-58, SE-10044 Stockholm, Sweden
[b] Instituto de Tecnología de Materiales (ITM), Escuela Técnica Superior de Ingeniería del Diseño (ETSID), Universidad Politécnica de Valencia Camino de Vera s/n, E-46022 Valencia, Spain
[c] School of Biotechnology, Division of Glycoscience, Royal Institute of Technology, Albanova University Centre, SE-10691 Stockholm, Sweden
[d] Wallenberg Wood Science Centre (WWSC), Teknikringen 56-58, SE-10044 Stockholm, Sweden
[e] University of Skövde, Box 408, SE-541 28 Skövde, Sweden

ARTICLE INFO

Article history:
Received 21 January 2014
Received in revised form 4 June 2014
Accepted 6 June 2014
Available online 13 June 2014

Keywords:
Natural fibres
Cellulose
Hemicellulose
Lignin
Crystalline content
Thermal properties

ABSTRACT

The potential of lignocellulosic natural fibres as renewable resources for thermal conversion and material reinforcement is largely dependent on the correlation between their chemical composition, crystalline structure and thermal decomposition properties. Significant differences were observed in the chemical composition of cotton, flax, hemp, kenaf and jute natural fibres in terms of cellulose, hemicellulose and lignin content, which influence their morphology, thermal properties and pyrolysis product distribution. A suitable methodology to study the kinetics of the thermal decomposition process of lignocellulosic fibres is proposed combining different models (Friedman, Flynn–Wall–Ozawa, Criado and Coats–Redfern). Cellulose pyrolysis can be modelled with similar kinetic parameters for all the natural fibres whereas the kinetic parameters for hemicellulose pyrolysis show intrinsic differences that can be assigned to the heterogeneous hemicellulose sugar composition in each natural fibre. This study provides the ground to critically select the most promising fibres to be used either for biofuel or material applications.

1. Introduction

Natural fibres are promising raw materials in thermo-chemical/biochemical conversion plants for bioenergy and as reinforcement agents in biocomposites. Renewable biomass has become increasingly recognized as a sustainable substitute to fossil resources for natural fuel, heat or power production. On the other hand, natural fibres are emerging as a viable alternative to glass fibres as reinforcements in thermoplastics and they are becoming one of the fastest growing polymer additive in the composite industry and, therefore in the biomaterial sector (Mohanty, Misra, & Drzal, 2005). Biomass natural fibres have many significant advantages over fossil resources: renewability, sustainability, no impact on global warming, low cost, biodegradability, non-abrasive properties during processing and mechanical properties comparable to glass fibres (Fowler, Hughes, & Elias, 2006; Mohanty, Misra, & Hinrichsen, 2000). However, they have some drawbacks that should be considered. The characteristic properties of natural fibres vary considerably depending on their origin (seed, bast, leaf and fruit), the plant location and their age, whereas the products from fossil resources can be produced with a narrow range of properties (Mohanty, Misra, & Drzal, 2002). In general, cotton constitutes the largest non-woody plant fibre in terms of production and consumption, although flax, hemp, jute, kenaf, bamboo, sisal and coconut fibres are also widely employed. The most common fibres applied as reinforcements in composites have been flax, hemp, jute and kenaf. Hemp and kenaf fibres have also been proposed as alternative renewable resources to produce biofuel, biodiesel or bioalcohol; however, common practice is still on the domain of woody natural fibres (Fiore, Scalici, & Valenza, 2014). The use of non-woody natural fibres for bioenergy and biomaterials is however hindered by their heterogeneity and the lack of knowledge about their chemical, structural and thermo-mechanical properties. Correlating their complex composition and structure with their functional properties is decisive to assess their potential as renewable resources for

* Corresponding author at: Division of Wood Chemistry and Pulp Technology, School of Chemical Science and Engineering, KTH Royal Institute of Technology, Teknikringen 56, SE-10044 Stockholm, Sweden. Tel.: +4687908067; fax: +46 87906166.
E-mail addresses: rosana@kth.se, romotor@hotmail.com (R. Moriana).

http://dx.doi.org/10.1016/j.carbpol.2014.06.009
0144-8617/

their sustainable exploitation (Satyanarayana et al., 1986). All natural fibres are composed of three main constituents: cellulose, lignin and matrix polysaccharides (such as pectins and hemicelluloses), associated with cellulose and lignin in the cell wall forming a heterogeneous network. Each fibril has a complex layered structure consisting of a thin primary wall and a secondary wall that is made up of three layers. The middle layer of this secondary wall consists of a series of helically wound cellular microfibrils of about 10–30 nm of diameter formed by long chain cellulose molecules. The amorphous matrix phase in a secondary cell wall consists of hemicellulose, lignin, and in some cases pectin. Therefore, natural fibres can be considered to be hollow composites of crystalline cellulose fibrils held together by a lignin and hemicellulose matrix (Jayaraman, 2003). The crystalline nature of naturally occurring cellulose is known as cellulose I. This native cellulose occurs in different crystalline allomorphs: cellulose Iα assigned to one-chain triclinic unit cell and cellulose Iβ assigned to two-chain monoclinic unit cell (John & Thomas, 2008). The numerous strongly polar groups make cellulose molecules predestined for building up hydrogen bonds within the molecule and between different molecules. In the generally accepted structure of cellulose I, intermolecular hydrogen bonds of type 6-OH···O-3 and intramolecular hydrogen bonds of types 2-OH···O-6 and 3-OH···O-5 are present for both sides of the chain (Barton, Nakanishi, & Meth-Cohn, 1999). The hydrogen-bonding pattern varies for the different cellulose allomorphs influencing the mechanical and conformational properties (O'Sullivan, 1997).

The thermal stability, the thermal degradation kinetics and the pyrolysis product distribution are other important concerns for processing and using natural fibre as raw materials to produce biomaterials or bioenergy. It is therefore of practical significance to understand and predict the thermal properties of natural fibre constituents for the rational design of biomass conversion and material processing technologies. The thermal degradation kinetics is interpreted on the basis of the kinetic triplet: activation energy, pre-exponential factor and the reaction model or reaction mechanisms. Their evaluation provides accurate prediction of the biomass behaviour under different thermal conditions that will be useful for their processing/conversion and later specific applications. Due to the complexity of thermal decomposition reactions of natural fibres, the suitable kinetic model for natural fibres remains under discussion (Capart, Khezami, & Burnharm, 2004). The "model-free" iso-conversional methods are considered as a helpful solution for truly determining kinetic parameters without making any assumptions about the reaction mechanisms (Maciejewski, 2000). Here we propose an integrated methodology using iso-conversional methods to assess the kinetic triplet. Moreover, we correlate the chemical composition and the pyrolysis characteristics for cotton, flax, hemp, jute and kenaf fibres with their thermal and structural properties, in order to draw important implications for their future application as reinforcements in polymer-based composites and as bioresources for biomass-energy conversion processes.

2. Materials and methods

2.1. Materials

Cotton, flax, hemp, kenaf and jute were the selected biomass natural fibres, provided by Yute S.L. (Spain). Table 1 shows the average Young moduli of each natural fibre provided for the manufacturer and calculated following the ASTM-D3822. The average length and diameter of each natural fibre have been determined by optical microscopy (Olympus CH30 Microscope, USA) over 200 fibres. The aspect ratio was calculated by dividing the fibre length of each natural fibre by its diameter and the resulting parameters are also summarized in Table 1.

2.2. Chemical composition analysis

The chemical composition of each natural fibre was calculated following the same procedure as reported in previous works (Moriana, Vilaplana, Karlsson, & Ribes-Greus, 2011). The sugar composition was determined after derivatization into their alditol acetates by gas chromatography (GC) using a Hewlett-Packard HP-6890 chromatograph. Inositol was used as an internal standard. Separation was performed in a BP X70 capillary column with dimensions 12 m × 0.32 mm ID (SGE Analytical Science) operated at 210 °C with helium as the carrier gas. The injector temperature was kept at 250 °C and the detector temperature was 230 °C. A mixture of standards (glucose, mannose, xylose, arabinose and galactose) were used to elaborate the calibration curves. The Klason lignin content was measured after acid hydrolysis with 72% H_2SO_4, according to the standard procedures of Tappi test method T222 om-06 (TAPPI, 2006). The ash content was determined after pyrolysis of the dry sample in a furnace at 525 °C during 6 h, following the standard procedure of Tappi test method T211 om-02 (TAPPI, 2012). The humidity of the samples was calculated using a Mettler Toledo HB43 moisture analyser (Columbus, OH). Two replications of each natural fibre were performed and averaged, the deviations from the average were considered.

2.3. Fourier-transform infrared spectrometry

Fourier-transform infrared spectrometry (FTIR) was used to analyse the chemical structure and to obtain morphologic information from the functional groups related to the cellulose crystalline domains. FTIR spectra were recorded at room temperature, in a FTIR Spectrum 2000 spectrometer from Perkin Elmer (Wellesley, MA), equipped with a golden gate single-reflection diamond accessory for ATR measurements. Each spectrum resulted from the performance of 24 scans between 4000 and 600 cm^{-1} at intervals of 1 cm^{-1} with a resolution of 4 cm^{-1}. The spectra were automatically baseline-corrected and smoothened using Omnic 7 Software. The measurements were repeated seven times to assure their accuracy. The average and the standard deviation from these measurements were considered to calculate the experimental parameters. The relative contents of the crystalline allomorph of each natural fibre were identified using the second derivatives of the FTIR spectra.

2.4. Wide angle X-ray scattering

The natural fibres were analysed at ambient temperature on an X-ray diffractometer (X'Pert PRO MPD PANalytical, The Netherlands) using a monochromatic CuKa radiation (λ = 1.54 Å) in the range of 2θ = 10–40° with a scanning rate of 1.0° min^{-1}. The X-ray unit was operated at 40 kV and 35 mA. The crystalline index (CI) of the cellulose in each natural fibre was assessed using the Segal empirical method (Segal, Creely, Martin, & Conrad, 1959) after subtraction of the background signal:

$$\mathrm{CrI}\,(\%) = \frac{I_{002} - I_{\mathrm{AM}}}{I_{002}} \times 100 \quad (1)$$

where I_{002} is the counter reading at peak intensity at 2θ angle close to 22.5° and I_{AM} is amorphous counter reading at 2θ angle between 18° and 19° where the intensity is at a minimum.

2.5. Thermal analysis

The thermal decomposition of the natural fibres was evaluated by thermogravimetric analysis (TGA). The thermogravimetric data

Table 1
Morphological, physical and mechanical properties of the natural fibres.

	Cr I			HBI	Average length (mm)	Average diameter (μm)	Aspect ratio	E-modulus (GPa)
	A1371/A665	H1371/H2900	$(I_{002}-I_{AM})/I_{002}$	H4000-2995/H1337				
Cotton	6.02 ± 0.3	0.50 ± 0.02	0.54 ± 0.1	16.25 ± 0.5	3.0 ± 1.0	18 ± 2	66.7–666.7	12.0 ± 4.0
Flax	6.96 ± 0.3	0.53 ± 0.02	0.62 ± 0.1	17.98 ± 0.6	6.0 ± 4.0	20 ± 3	136.6–500.0	60.0 ± 1.0
Hemp	5.01 ± 0.2	0.43 ± 0.02	0.51 ± 0.1	14.26 ± 0.5	1.0 ± 0.5	27 ± 2	150.7–214.0	50.0 ± 5.0
Kenaf	4.94 ± 0.2	0.36 ± 0.03	0.45 ± 0.2	13.35 ± 0.3	10.0 ± 5.0	150 ± 5	25.0–150.0	40.0 ± 5.0
Jute	7.64 ± 0.3	0.66 ± 0.03	0.73 ± 0.1	18.89 ± 0.3	6.5 ± 3.5	10 ± 3	230.7–1428.5	70.0 ± 1.5

were obtained from a TGA Mettler-Toledo 851 module (Columbus, OH) under argon atmosphere (50 ml/min), at different heating rates (3–30 °C/min) in a temperature range between 25 and 750 °C. A deconvolution method based on an asymmetrical model that was successfully applied in previous works (Moriana et al., 2011) was employed in this work to separate the main thermal decomposition processes. The mass-loss percentages, the onset (initial decomposition temperature), the peak temperature (temperature at maximum decomposition rate) and the endset (temperature at involution peak) were calculated using STAR^e Evaluation Software (Mettler-Toledo, Columbus, OH). The measurements were performed at least four times; the average and the average deviation from these data were considered as representative.

2.6. Thermal degradation kinetics

An integrated methodology is proposed to evaluate the thermal degradation kinetics of the natural fibres by means of the determination of the kinetic triplet, which includes the apparent activation energy (*Ea*), the reaction mechanism ($f(\alpha)$) and the pre-exponential factor (*A*) of each individual thermal decomposition process. The proposed methodology to analyse the kinetic parameters of each thermal decomposition process was carefully checked: differential and integral iso-conversional methods of Friedman (Friedman, 1983) and Flynn–Wall–Ozawa (Ozawa, 1965) were firstly used to determine the apparent activation energy (*Ea*); discussion of the probable reaction model was based on Criado method (Criado, 1978); and Coats–Redfern equation (Coats & Redfern, 1964) was used to calculate the different *Ea* from the identified Criado kinetic models and to select the most suitable $f(\alpha)$, to latter determine the pre-exponential factor (*A*). Table 2 details the different equations of each employed thermal degradation kinetic method.

3. Results and discussion

3.1. Chemical composition analysis

The carbohydrate composition of the natural fibres was determined from the quantification of the area peaks from chromatographic curves corresponding to the glucose, mannose, xylose, arabinose and galactose of each natural fibre. Table 3 shows the natural fibres carbohydrate composition in terms of relative percentage, taking into account the ash and humidity percentages. The amount of cellulose results from the percentage of glucose, whereas the amount of hemicellulose/pectin corresponds to the percentage of the remaining sugars. Some hemicelluloses may contain as well glucose monomers in their structure (e.g. glucomannans) but their contribution is somewhat minor in secondary cell walls compared to cellulose, as it can be observed in the low mannose content from Table 3. As it was expected, the studied natural fibres present important differences in their chemical composition. Cotton fibres have the highest cellulose content (91.5%) and the lowest lignin content. Kenaf fibres present the highest content in hemicelluloses/pectins (22.0%) and lignin (11.8%), and the lowest ash content (1.2%). Flax fibres present the lowest lignin content (2.8%) and the highest ash percentage (7%). In addition, from these values, a direct relation can be observed between the humidity and the hemicellulose/pectin percentages (Fig. 1a), evidencing the humidity content of each natural fibre depends of the most hydrophilic component present in the natural fibres, this is, hemicellulose/pectin.

Table 1 displays the fibres with highest cellulose content (cotton, flax and jute) can offer the highest aspect ratio and therefore should mean a greater reinforcing efficacy in composites (Fowler et al., 2006). It is thought that higher cellulose content means also higher E-modulus (Mohanty et al., 2002). However, only the bast fibres (flax and jute) with the highest content of cellulose and highest aspect ratio display the highest E-modulus. Hence, it is not possible to correlate the fibre E-modulus with cellulose content without taking into account other aspects (such as the source of fibre) that can influence on their very complex structure (Mohanty et al., 2000). Considering this mechanical property is possible to state the two bast fibres with the highest cellulose content could be considered as potentially competitive with the glass and aramid fibres that have a modulus of 70–75 (Fowler et al., 2006) and 63–67 GPa (Mohanty et al., 2000), respectively.

3.2. Fourier-transform infrared spectrometry

FTIR is sensitive to different conformations and local molecular environments of the cellulose molecules, which make them suitable for determination of cellulose allomorphs and hydrogen-bonding patterns (Olsson & Salmén, 2004). The FTIR spectra of all the natural fibres were recorded and different characteristic bands were identified. Three bands placed around 3435 cm^{-1}, 3339 cm^{-1} and 3292 cm^{-1} were observed in the region related to hydrogen-bonded OH stretching (Proniewicz et al., 2001). Cotton fibres showed a predominant number of intermolecular hydrogen bonding of 6OH···O3 in their structure, whereas flax, hemp, kenaf and jute fibres displayed a predominant intramolecular hydrogen bonding of 3OH···O5. Furthermore, these five fibres showed differences in the region of the C—H stretching vibrations that could be related to the different amount of the chemical constituents of each natural fibre. Cotton and jute fibres showed a single peak at 2899 and 2890 cm^{-1}, respectively, both related to the C—H stretching vibrations of cellulose, whereas kenaf, flax and hemp fibres showed a doublet at 2920 cm^{-1} and 2850 cm^{-1}, attributed to the anti-symmetrical and symmetrical CH_2 stretching vibrations of non-cellulose polysaccharides (Andreeva, Burkova, Grebenkin, & Grebenkin, 2002), respectively. Different intensities in the bands placed around 1640 cm^{-1} attributed to the OH bending mode of water (Hinterstoisser & Salmen, 1999), can be also observed in all natural fibres. He, Tang, and Wang (2007) proposed the use of the peak ratio between 1640 and 2900 cm^{-1} to determine the moisture index of each natural fibre (MI). Fig. 1b displays the moisture index of each natural fibre as a function of the hemicellulose/pectin composition; a linear increase of the moisture index with the hemicellulose/pectin percentage can be also observed. These results agree with those displayed in the chemical composition and confirming that kenaf and jute fibres have the highest moisture index due to the highest hemicellulose/pectin content.

Table 2
Mathematical definition of the thermal degradation kinetic methods employed in our methodology.

Methods	Expression	Plots	
Friedman	$\ln\left(\frac{d\alpha}{dt}\right) = \ln\ A \cdot f(\alpha) - \frac{Ea}{R \cdot T}$	$\ln\left(\frac{d\alpha}{dt}\right)$ vs. $1/T$	α – conversion degree A – pre-exponential factor Ea – apparent activation energy
Flynn–Wall–Ozawa	$\log\ \beta = \log\frac{A \cdot Ea}{g(\alpha) \cdot R} - 2.315 - 0.45\left(\frac{Ea}{R \cdot T}\right)$	$\log\beta$ vs. $1/T$	T – absolute temperature R – gas constant β – heating rate
Criado	$\frac{z(\alpha)}{z(0.5)} = \frac{f(\alpha)g(\alpha)}{f(0.5)g(0.5)} = \left(\frac{T}{T_{0.5}}\right)^2 \frac{(d\alpha/dt)}{(d\alpha/dt)_{0.5}}$	$\frac{z(\alpha)}{z(0.5)}$ vs. α, $\left(\frac{T}{T_{0.5}}\right)^2 \frac{(d\alpha/dt)}{(d\alpha/dt)_{0.5}}$ vs. α	$g(\alpha)$ – integral conversion function 0.5 – refers to $\alpha = 0.5$.
Coats–Redfern	$\ln\frac{g(\alpha)}{T^2} = \ln\frac{A \cdot R}{\beta \cdot Ea} - \frac{Ea}{R \cdot T}$	$\ln\frac{g(\alpha)}{T^2}$ vs. $1/T$	t – absolute time

Table 3
Chemical composition of the natural fibres.

	Arabinose (%)	Mannose (%)	Xylose (%)	Galactose (%)	Glucose (%)	Hemicellulose/pectin (%)	Cellulose (%)	Lignin (%)	Ash (%)	Humidity (%)
Cotton	0.6 ± 0.2	0.5 ± 0.2	0.8 ± 0.2	0.4 ± 0.2	91.5 ± 0.5	2.3 ± 0.2	91.5 ± 0.5	–	2.0 ± 0.2	4.0 ± 0.2
Flax	0.7 ± 0.2	1.3 ± 0.2	6.3 ± 0.2	0.4 ± 0.2	77.0 ± 0.3	8.7 ± 0.2	77.0 ± 0.3	2.8 ± 0.5	7.0 ± 0.5	4.5 ± 0.2
Hemp	3.3 ± 0.2	5.1 ± 0.2	2.5 ± 0.2	2.1 ± 0.2	69.3 ± 0.2	13.0 ± 0.2	69.4 ± 0.2	5.7 ± 0.3	5.8 ± 0.5	5.1 ± 0.3
Kenaf	0.7 ± 0.2	1.9 ± 0.3	18.1 ± 0.2	1.3 ± 0.3	57.6 ± 0.5	22.0 ± 0.2	57.6 ± 0.5	11.8 ± 0.5	1.2 ± 0.2	7.0 ± 0.4
Jute	0.5 ± 0.2	0.4 ± 0.2	10.2 ± 0.2	3.0 ± 0.2	71.5 ± 0.3	14.1 ± 0.2	71.5 ± 0.3	6.4 ± 0.5	2.5 ± 0.2	5.5 ± 0.2

The degree of crystallinity can be estimated by infrared spectroscopy using some empirical parameters, such as the crystallinity index (CrI) and the hydrogen-bond intensity (HBI). These parameters are defined as a function of the relative intensity of certain bands (at 4000–2995 cm^{-1}, 2900 cm^{-1}, 1430 cm^{-1}, 1370 cm^{-1}, and 900 cm^{-1}) that are especially sensitive to the crystalline and amorphous regions in the cellulose. The empirical parameters used to assess the degree of crystallinity are:

(i) The ratio of the absorbance height of the maximum peak between 4000 and 2990 cm^{-1} and 1337 cm^{-1} (H4000-2990/H1337) as an empirical HBI parameter (Nada, Kamel, & Sakhawy, 2000).
(ii) The absorbance ratio H1371/H2900 and the area ratio A1371/A665 as an empirical crystallinity index parameter (CrI) (Arkerholm, Hinterstoisser, & Salmen, 2004).

Table 1 summarizes the values of crystalline index and hydrogen-bond intensity for all natural fibres. The CrI values and the HBI follow the same trend for the five fibres. Kenaf and hemp with lower cellulose percentages exhibit lower crystalline features than jute, flax and cotton fibres with higher cellulose content. However, it should be pointed out the fact that cotton shows lower CrI and HBI values than jute and flax despite of being the natural fibre with the highest cellulose content. This could be due to the fact that cotton fibres have more amorphous cellulose in their composition.

The second derivative of the FTIR spectra (Fig. 2) allows the investigation of the crystalline allomorphs present in the natural fibres, by enhancing the resolution of the OH stretching group (Proniewicz et al., 2001). The bands at 3268 and 710 cm^{-1} are characteristic of the I_β crystalline phase (Kokot, Czarnik, & Ozaki, 2002), whereas the bands at 3230 cm^{-1} and 750 cm^{-1} identify the I_α crystalline phase (Kokot et al., 2002). The higher relative intensity of the bands related to the I_β phase in all the natural fibres indicates that the cellulose in these natural fibres consists mainly of I_β phase (Larsson, Westermark, & Iversen, 1995). Jute, flax and cotton fibres have the highest intensity of the bands at 3270 and 710 cm^{-1} and therefore the highest I_β allomorph content.

3.3. Wide angle X-ray scattering

All the natural fibres showed the typical X-ray diffractogram features of cellulose I. The major diffraction peaks of cellulose 1 0 1, 1 0 1, 0 2 1, 0 0 2 and 0 4 0 were present around 14.6, 16.8, 20.6, 22.4 and 34.7 2θ angle (Quajai & Shanks, 2005). The X-ray diffractograms from kenaf and jute fibres are given in Fig. 3, where it can be observed that the major crystalline peak of jute fibres is much higher than that of kenaf. Table 1 summarizes the values of

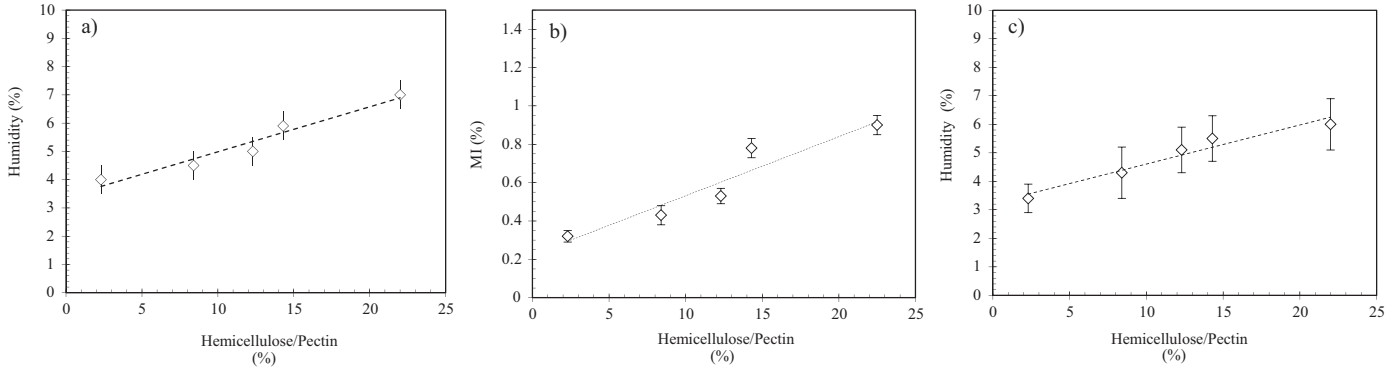

Fig. 1. (a) Humidity percentage and (b) index of moisture content as a function of the hemicellulose and pectin content calculated by chemical analysis, (c) humidity percentage as a function of the hemicellulose and pectin content calculated by thermogravimetric analysis.

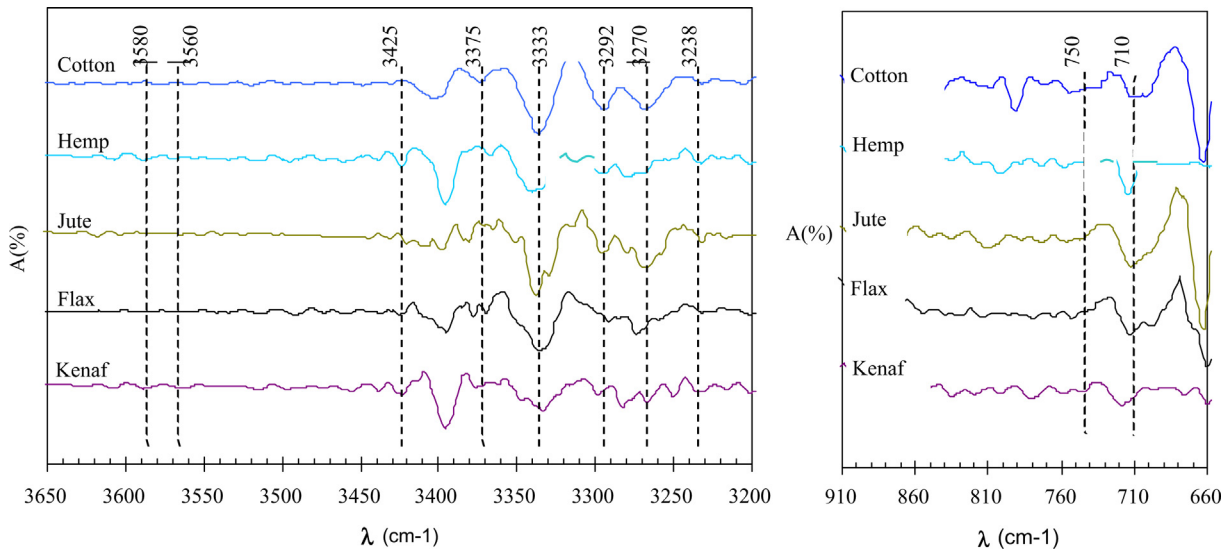

Fig. 2. Second derivative FTIR spectra for natural fibres.

crystalline index for all natural fibres. These results are in good agreement with those previously published (Bhatnagar & Sain, 2005; Dai & Fan, 2010; Ford, Sharathkumar, Thames, & Rawlins, 2010; Leonard & Martin, 2002). The X-ray crystalline index (CrI) values follow the same trend as in FTIR analysis for the five fibres. Kenaf and hemp with lower cellulose content exhibit lower crystalline index than jute, flax and cotton fibres with higher cellulose content.

3.4. Thermal analysis

The thermal degradation of the natural fibres was analysed in detail by dynamical thermogravimetry at different heating rates. Several mass-loss regions can be observed for the pyrolysis of natural fibres (Fig. 4); similar patterns are obtained at different heating rates (Fig. 5a). As it was expected, the onset and the temperature peak increase as a function of the heating rate, whereas the mass-loss percentages and the residue content are not significantly influenced (Willium & Besler, 1996). The first mass-loss region between 25 and 145 °C is attributed to the water absorption (Mamleev, Bourbigot, & Yvon, 2007) and it is found that this percentage increases as a function of the hemicellulose/pectin content with a good regression (Fig. 1c) and a similar slope as that showed in Fig. 1a. The second mass-loss region (from 200 to 550 °C) shows a complex thermal decomposition process with a main peak placed around 350 °C associated to the thermal decomposition of cellulose (Aggarwal, Dollimore, & Heon, 1997). An overlapping shoulder related to the pyrolysis of both hemicellulose and pectin appears at lower temperatures (lower than 325 °C) (Yao, Wu, Lei, Guou & Xu, 2008) and a tail is displayed above 367 °C, which is related to the degradation of lignin (Evans & Milne, 1987) and to the volatilization of the char that was obtained previously during the cellulose, hemicellulose and lignin degradation (Barneto, Carmona, Alfonso, & Sánchez-Serrano, 2010). The individual contributions of the overlapped processes in this second mass-loss region, corresponding to hemicellulose/pectin (*peak H*), cellulose (*peak C*) and high temperature tail (*peak T*), were determined using a deconvolution procedure based on an asymmetrical model that was previously used to separate the main peaks of the DTG curves of cotton, hemp and kenaf (Moriana et al., 2011). According to Barneto et al. (2010), the char volatilization should be taken into account to avoid overestimation of the lignin decomposition in the high temperature tail. Therefore, in this work we extended the previous analyses by resolving two new contributions in the region where the mass-loss associated to lignin and char is occurring: one at lower temperatures (<400 °C) related with the lignin decomposition (*peak TL*); and another at higher temperatures (>400 °C) related to the char (*peak TC*). The results of the fitting procedure for the deconvolution of the thermal decomposition processes for the natural fibres are displayed in Fig. 4. The hemicellulose/pectin, cellulose and lignin percentages from the chemical analysis were compared to the relative ML_H, ML_C and ML_{TL} dates from the thermogravimetric analysis (*without taking into account the residue, the char and the humidity content*) (Table 4). These results confirm that the proposed thermogravimetric methodology can be used as a fast tool to screen the chemical composition of lignocellulosic materials.

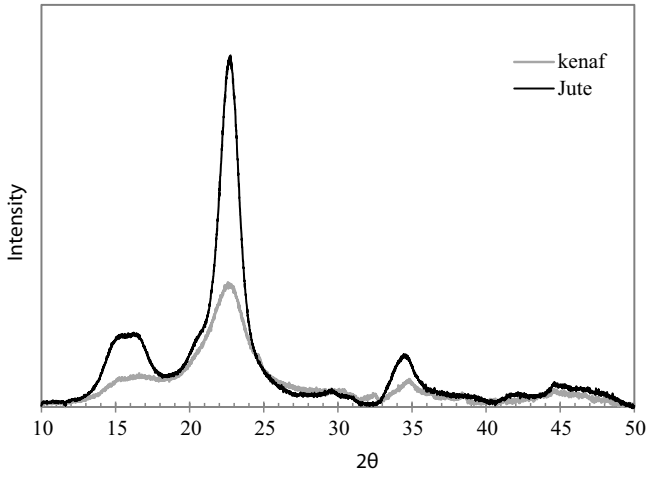

Fig. 3. X-ray diffraction of kenaf and jute fibres.

Thermogravimetric analysis has been widely employed in the last decades for the determination of the pyrolysis characteristics and product distribution of biomass (Barneto et al., 2010). The pyrolysis can be understood as a biomass conversion technology that allows the devolatization of volatile matter in inert medium to produce pyrolytic liquids (tar, high molecular hydrocarbons and water), solid char (fixed carbon) and gaseous products (Kirubakaran, Sivaramakrishnana, Sekar, Premalatha, & Subramanian, 2009). The gaseous fuel has a high content in hydrocarbons with high calorific values and the solid char may be used

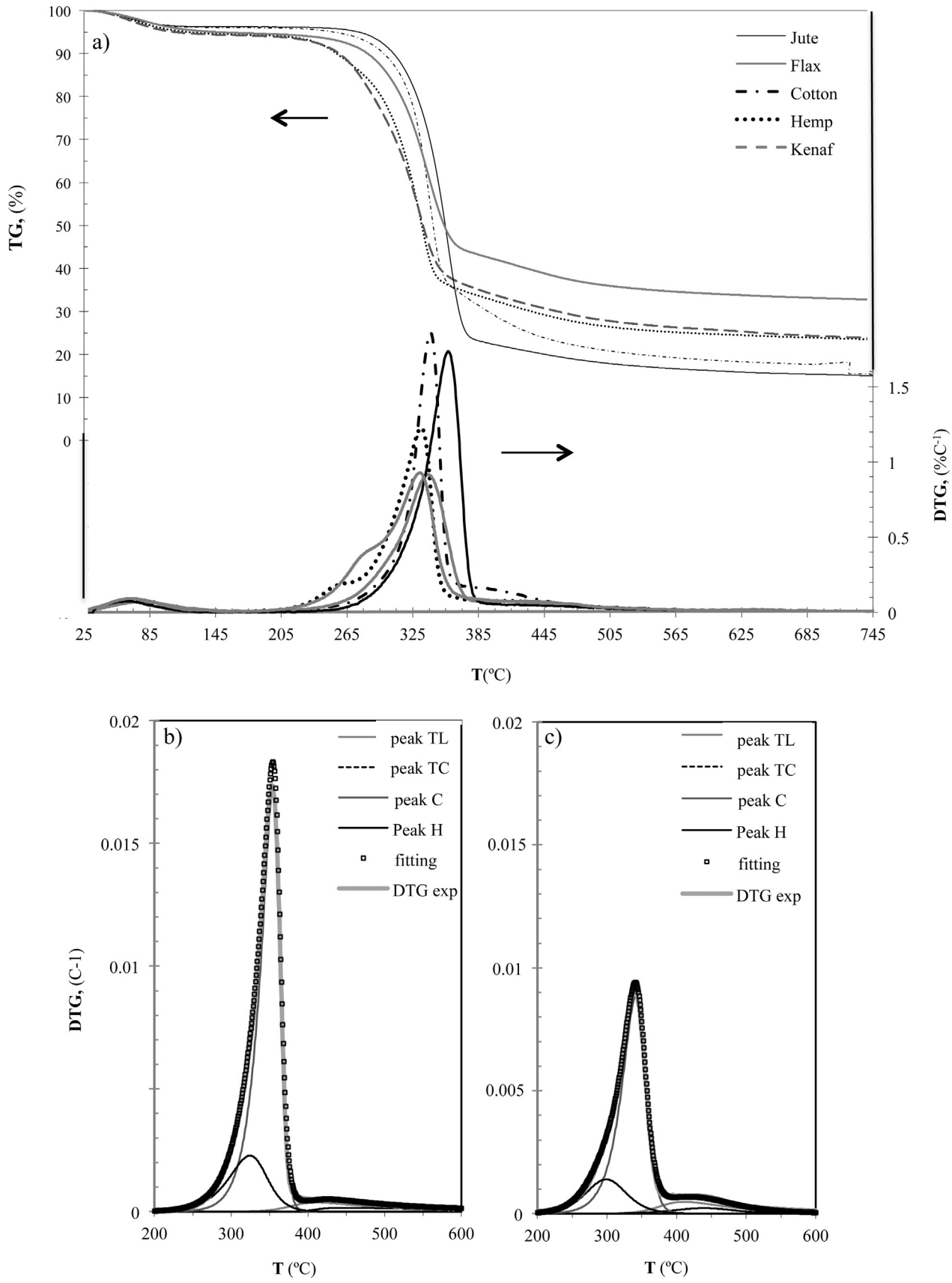

Fig. 4. (a) Thermogravimetric (TG) and derivative curves (DTG) for the natural fibres at 5 °C/min, DTG fitting curves of (b) flax and (c) jute fibres.

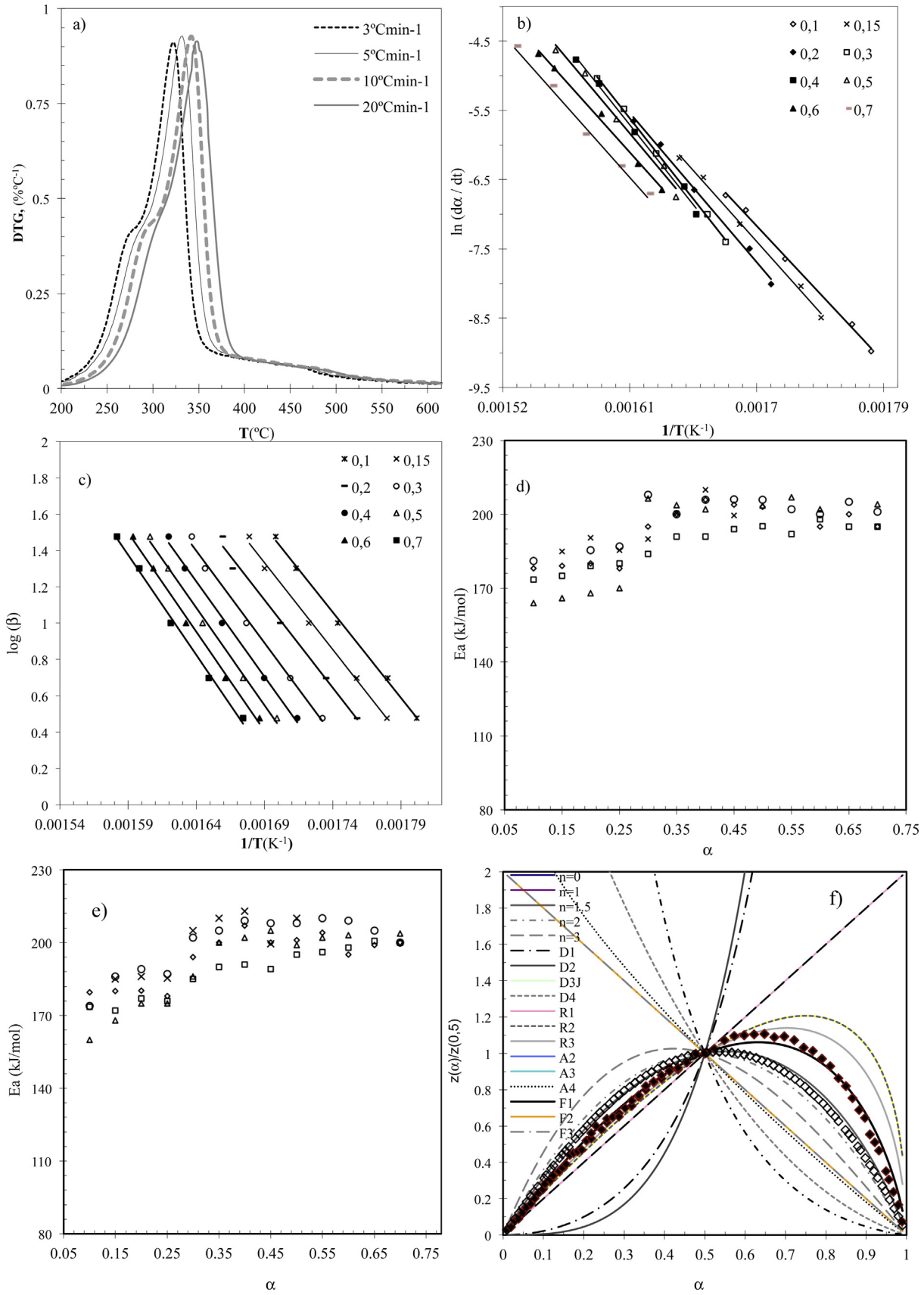

Fig. 5. (a) DTG curves for the kenaf fibres at different heating rates, (b) Friedman curves for hemp fibres, (c) Flynn–Wall–Ozawa curves for jute fibres, (d) Friedman *Ea* values for ○: cotton; ◊: flax; ×: hemp; □: kenaf and Δ: jute fibres, (d) Flynn–Wall–Ozawa *Ea* values for ○: cotton; ◊: flax; ×: hemp, □: kenaf and Δ: jute fibres, (e) Criado curves for flax fibres ◊: hemicellulose/pectin region and ■:cellulose region.

Table 4
Comparative results of the composition of the natural fibres between the chemical analysis and the thermogravimetric results.

	Hemicellulose/pectin (%)		Cellulose (%)		Lignin (%)	
	CA[a]	TGA[b]	CA[a]	TGA[b]	CA[a]	TGA[b]
Cotton	2.5	2.7	97.4	96.7	–	–
Flax	9.6	9.3	87.2	88.1	3.2	4.2
Hemp	14.2	14.1	79.0	80.3	6.6	6.0
Kenaf	24.3	23.9	63.4	63.4	12.2	12.6
Jute	15.2	15.1	78.0	77.3	6.8	7.3

[a] Carbohydrate analysis.
[b] Thermogravimetric analysis.

as a starting material for fuel production. Table 5 reports the pyrolysis characteristics of the natural fibres in terms of volatile matter and fixed carbon. Over 60% of biomass decomposes into the volatile fraction in all the studied natural fibres, reaching more than 80% in the case of the jute and cotton fibres. This biomass devolatization corresponds to the second mass-loss at temperatures between 200 and 550 °C, where a remarkable slope of the TG curves is observed, due to the liberation of volatile hydrocarbon from the thermal decomposition of biomass. This shows that volatile products play a very important role in biomass pyrolysis and product gas composition (Abdullah, Yusup, Ahmad, Ramli, & Ismail, 2010). On the other hand, flax, hemp and kenaf show the highest amount of fixed carbon and therefore, higher potential to be used as a bioresources in the low temperature carbonization and slow pyrolysis technologies. The changes in the maximum rate pyrolysis and degradation temperatures (onset, peak temperature and endset) were also studied (Table 5). The maximum decomposition rates for cotton and jute fibres are twofold as those for flax and kenaf fibres, suggesting higher reactivity at maximum decomposition temperature for these fibres. Considering the initial decomposition point (onset) a correlation with the previous crystalline index could be found: jute fibres display the highest onset, followed by cotton and flax fibres. Hemp and kenaf are the least thermal stable fibres with an onset value (~55 °C lower than flax) due to the lower content of crystalline cellulose that is the most thermal stable component of the lignocellulosic material (Barneto, Vila, Ariza, & Vidal, 2011). In general, the natural fibres with higher cellulose content exhibit improved thermal stability, which is very attractive when used as reinforcements in composites due to their resistance to degradation during processing or service life. However, to evaluate the potential of these fibres as reinforcing agents in composites, the mechanical properties should be also considered (Mohanty et al., 2005). Jute and flax are the bast fibres with the highest cellulosic content, highest aspect ratio, highest crystallinity index, highest thermal and mechanical properties and, therefore the most attractive to be applied in composites. However, the remaining bast fibres with less percentage of cellulose and lower onset decomposition temperatures (kenaf and hemp) offer great potential as a resource for bioenergy, since lower operating temperatures will be required to start the thermal decomposition.

3.5. Thermal degradation kinetics

An integrated methodology is proposed to evaluate the thermal degradation kinetics of the natural fibres by means of the determination of the kinetic triplet. The Friedman and Flynn–Wall–Ozawa iso-conversional methods are considered as a helpful solution for determining the activation energy (*Ea*) without making any assumptions about the reaction mechanisms, assuming that the reaction rate only depends on the temperature and it is independent of the reaction mechanism. The Friedman and Flynn–Wall–Ozawa plots were performed for all the natural fibres (Fig. 5a and b). This assumption provided the basis of model-free methods where the *Ea* values are obtained as a function of the degree of conversion (α). The trend of *Ea* as a function of α for all the natural fibres by both isoconversional methods is displayed in Fig. 5c and d.

The isoconversional Friedman and Flynn–Wall–Ozawa methods offer an *Ea* range of approximate 150–205 kJ/mol for all the natural fibres in the studied conversion range. Activation energies change drastically from $\alpha = 0.1$ to $\alpha = 0.3$ and remain then quite stable at higher conversion. This indicates that the degradation mechanism at low conversion is different from that at high conversion, indicating the cleavage of linkages with different bond energies. Two different α intervals can be thus distinguished where the decomposition of one or several constituents are predominant. The temperature range where occurs the thermal decomposition process associated to hemicellulose/pectin presents a band range of 150–190 kJ/mol whereas the temperature range of the thermal cellulose decomposition remains almost constant around 190–205 kJ/mol for all studied fibres. The *Ea* found at higher conversion range ($0.3 \leq \alpha < 0.7$) are similar to those reported in literature (Varhegyi, Antal, & Szekely, 1988).

However, the average *Ea* values for the lower conversion in the range $0.1 \leq \alpha < 0.3$ are higher than those expected for the hemicellulose component (105–111 kJ/mol) (Gronli, Várhegyi, & Di Blasi, 2002). This fact could be due to the overlapped initial decomposition process of cellulose, which is attributed to the formation of ether bonds with an *Ea* of 90–179 kJ/mol (Mamleev et al., 2007). Table 6 summarizes the average *Ea* values of these two regions obtained by iso-conversional methods.

Due to the complex and overlapping thermal decomposition reactions of natural fibres, the suitable kinetic model for natural fibres remains to be developed (Capart et al., 2004). The scientific interest is currently focused on the determination of the individual decomposition behaviour of the main components in natural fibres (Yao et al., 2008). The DTG deconvoluted curves for the hemicellulose/pectin and cellulose components of each natural fibre were used as experimental data to be compared with the different kinetic models proposed by Criado (Fig. 4f). In parallel, Coats–Redfern method was used to calculate the apparent *Ea* from the different kinetic models proposed by Criado. These *Ea* values were compared with the ones obtained previously by iso-conversional methods, confirming the assumption of the reaction mechanisms for each component (Table 6). The lignocellulosic decomposition at lower degrees ($\alpha < 0.3$) follows a single-step mechanism of order *n* in all

Table 5
Pyrolytic properties of the natural fibres at 5 °C/min.

	Yield (w% db)		Max. rate (% °C^{-1})	Temp at max. rate (°C)	Onset (°C)	Endset (°C)
	Volatiles	Char[a]				
Cotton	80.2 ± 0.5	17.3 ± 0.5	1.9 ± 0.02	341.0 ± 0.4	287.9 ± 0.4	465.5 ± 0.2
Flax	64.7 ± 0.2	29.3 ± 0.6	0.9 ± 0.01	339.5 ± 0.2	279.9 ± 0.6	460.4 ± 0.6
Hemp	72.9 ± 0.2	20.8 ± 0.1	1.2 ± 0.03	333.7 ± 1.0	232.5 ± 2.6	435.3 ± 0.2
Kenaf	72.3 ± 0.5	26.8 ± 0.5	0.9 ± 0.01	332.7 ± 0.3	231.4 ± 1.0	439.4 ± 0.6
Jute	84.7 ± 0.2	16.7 ± 0.1	1.7 ± 0.03	354.6 ± 0.4	290.9 ± 0.3	465.5 ± 0.4

[a] Char or fixed carbon at 600 °C.

Table 6
Kinetic parameters for the thermal decomposition of cotton, hemp, kenaf, flax and jute fibres.

		Friedman	Flynn–Wall–Ozawa		Coats–Redfern and Criado		
		Ea (kJ/mol)	*A* (min^{-1})	*Ea* (kJ/mol)	*A* (min^{-1})	*Ea* (kJ/mol)	$f(\alpha)$
Cotton	$0.3 \leq \alpha < 0.7$	204 ± 3	$10^{15.0}$ ± 3	206 ± 3	$10^{15.6}$ ± 2	205 ± 2	$(1-\alpha)^1$
	$0.1 \leq \alpha < 0.3$	184 ± 3	$10^{11.0}$ ± 4	181 ± 4	$10^{11.0}$ ± 4	183 ± 3	$(1-\alpha)^{1.7}$
Flax	$0.3 \leq \alpha < 0.7$	201 ± 3	$10^{15.0}$ ± 3	200 ± 2	$10^{15.0}$ ± 4	202 ± 2	$(1-\alpha)^1$
	$0.1 \leq \alpha < 0.3$	177 ± 2	$10^{9.5}$ ± 2	178 ± 3	$10^{9.0}$ ± 3	177 ± 2	$(1-\alpha)^{1.5}$
Kenaf	$0.3 \leq \alpha < 0.7$	194 ± 3	$10^{14.8}$ ± 4	195 ± 3	$10^{14.8}$ ± 3	193 ± 2	$(1-\alpha)^1$
	$0.1 \leq \alpha < 0.3$	177 ± 3	$10^{9.0}$ ± 3	178 ± 4	$10^{8.9}$ ± 4	177 ± 3	$(1-\alpha)^1$
Hemp	$0.3 \leq \alpha < 0.7$	202 ± 3	$10^{14.9}$ ± 2	205 ± 3	$10^{14.0}$ ± 4	205 ± 3	$(1-\alpha)^1$
	$0.1 \leq \alpha < 0.3$	185 ± 2	$10^{11.0}$ ± 4	183 ± 4	$10^{11.4}$ ± 3	184 ± 4	$(1-\alpha)^{1.5}$
Jute	$0.3 \leq \alpha < 0.7$	203 ± 3	$10^{15.6}$ ± 3	202 ± 2	$10^{15.6}$ ± 2	202 ± 3	$(1-\alpha)^1$
	$0.1 \leq \alpha < 0.3$	168 ± 3	$10^{8.5}$ ± 2	171 ± 6	$10^{8.4}$ ± 4	169 ± 2	$(1-\alpha)^{1.2}$

the studied fibres. However, this region shows differences in the *Ea* (168–194 kJ/mol), A ($10^{8.4}$–$10^{11.4}$ min^1) and *n* (1–1.7) kinetic parameters for each natural fibre maybe due to the heterogeneous sugar composition of the hemicelluloses in each natural fibre. On the other hand, a first order mechanism ($n = 1$) for the decomposition kinetics of all natural fibres from a $0.3 \leq \alpha < 0.7$ range conversion where the pyrolysis of the cellulose is occurring (Bilbao, Arauzo, & Millera, 1987). This result suggests that cellulose pyrolysis is not influenced by the content of hemicellulose and lignin components. However the thermal decomposition kinetics of the hemicellulose component shows a different thermal behaviour for each natural fibre, evidencing that the thermal decomposition mechanisms depend on the inherent composition of the hemicellulose/pectin fraction in each natural fibre.

4. Conclusions

The proposed methodology assesses the potential of lignocellulosic fibres as natural resources for either thermal conversion or material reinforcements by correlating their composition, structure and macroscopic properties. A new thermogravimetric methodology has been proposed to analyse the thermal decomposition kinetics of lignocellulosic biomass and to assess their chemical composition. The proposed deconvolution method allows assessing the percentage of each chemical constituent of the natural fibres from the TGA data, opening up new possibilities for validating the obtained results from wet chemical analyses. Different inherent properties are required for each specific application; it is therefore important to correlate their compositional and structural parameters with their macroscopic properties in order to rationally design the processes and applications of these valuable renewable resources. The bast fibres with higher cellulose content (jute and flax) show higher structural properties and thermal stability, which makes them more suitable to be used as reinforcements in biocomposites. Contrarily, the fibres with the lowest cellulose content and thermal stability will offer beneficial pyrolysis processing conditions for bioenergy. These structure–property correlations will be very valuable to analyse the best available technology (BAT) and life cycle assessment (LCA) for natural fibres. The thermal kinetic results suggest that cellulose pyrolysis is not influenced by the content of hemicellulose and lignin components, however the thermal decomposition kinetics of hemicellulose depends on the type of natural fibre. This indicates the influence of the heterogeneous structure of hemicelluloses in terms of linkage and branching structure on the thermal decomposition.

Acknowledgements

FV thanks the Knut and Alice Wallenberg (KAW) Foundation for the support to his research position. The Spanish Ministry of Education is acknowledged for the concession of a pre-doctoral research position to Rosana Moriana through the FPI program.

References

Abdullah, S. S., Yusup, S., Ahmad, M. M., Ramli, A., & Ismail, L. (2010). *International Journal of Chemical and Biological Engineering*, *3*, 3.
Aggarwal, P., Dollimore, D., & Heon, K. (1997). *Journal of Thermal Analysis and Calorimetry*, *50*, 7.
Andreeva, Q. A., Burkova, L. A., Grebenkin, A. N., & Grebenkin, A. A. (2002). *Russian Journal of Applied Chemistry*, *75*, 1513.
Arkerholm, M., Hinterstoisser, B., & Salmen, L. (2004). *Carbohydrate Research*, *339*, 569.
Barneto, A. G., Carmona, J. A., Alfonso, J. E., & Sánchez-Serrano, R. (2010). *Bioresource Technology*, *10*, 3220.
Barneto, A. G., Vila, C., Ariza, J., & Vidal, T. (2011). *Cellulose*, *18*, 17.
Barton, D., Nakanishi, K., & Meth-Cohn, O. (1999). *Celluloses* (first edition). Oxford: Elsevier Science.
Bhatnagar, A., & Sain, M. (2005). *Journal of Reinforced Plastics and Composites*, *24*, 1259.
Bilbao, R., Arauzo, J., & Millera, A. (1987). *Thermochimica Acta*, *120*, 121.
Capart, R., Khezami, L., & Burnharm, A. K. (2004). *Thermochimica Acta*, *417*, 79.
Coats, A. W., & Redfern, J. P. (1964). *Nature*, *201*, 68.
Criado, J. M. (1978). *Thermochimica Acta*, *24*, 86.
Dai, D., & Fan, M. (2010). *Materials Science and Applications*, *1*, 336.
Evans, R. J., & Milne, T. A. (1987). *Energy & Fuels*, *1*, 123.
Fiore, V., Scalici, T., & Valenza, A. (2014). *Carbohydrate Polymers*, *106*, 77.
Ford, E. N. J., Sharathkumar, K. M., Thames, S. F., & Rawlins, J. W. (2010). *Journal of Engineered Fibers and Fabrics*, *5*, 1.
Fowler, P. A., Hughes, J. M., & Elias, R. M. (2006). *Journal of the Science of Food and Agriculture*, *86*, 1781.
Friedman, H. L. (1983). *Journal of Polymer Science*, *6*, 183.
Gronli, M. G., Várhegyi, G., & Di Blasi, C. (2002). *Industrial & Engineering Chemistry Research*, *41*, 4201.
He, J., Tang, Y., & Wang, S. Y. (2007). *Iranian Polymer Journal*, *16*, 807.
Hinterstoisser, B., & Salmen, L. (1999). *Cellulose*, *6*, 251.
Jayaraman, K. (2003). *Composites Science and Technology*, *63*, 367.
John, M. J., & Thomas, S. (2008). Biofibres and biocomposites. *Carbohydrate Polymers*, *71*, 343.
Kirubakaran, V., Sivaramakrishnana, N. R., Sekar, T., Premalatha, M., & Subramanian, P. (2009). *Renewable and Sustainable Energy Reviews*, *13*, 179.
Kokot, S., Czarnik, B., & Ozaki, Y. (2002). *Biopolymers*, *67*, 456.
Larsson, P. T., Westermark, U., & Iversen, T. (1995). *Carbohydrate Research*, *278*, 24.
Leonard, Y. M., & Martin, P. A. (2002). *Journal of Applied Polymer Science*, *84*, 222.
Maciejewski, M. (2000). *Thermochimica Acta*, *355*, 145.
Mamleev, V., Bourbigot, S., & Yvon, J. (2007). *Journal of Analytical and Applied Pyrolysis*, *80*, 151.
Mohanty, A. K., Misra, M., & Drzal, T. D. (2005). *Natural fibers, biopolymers and biocomposites*. Boca Raton: Taylor & Francis.
Mohanty, A. K., Misra, M., & Drzal, T. D. (2002). *Journal of Polymers and the Environment*, *10*(1/2.).
Mohanty, A. K., Misra, M., & Hinrichsen, G. (2000). *Macromolecular Materials and Engineering*, *276/277*, 1.
Moriana, R., Vilaplana, F., Karlsson, S., & Ribes-Greus, A. (2011). *Composites Part A: Applied Science and Manufacturing*, *42*, 30.
Nada, A. M., Kamel, S., & Sakhawy, M. E. (2000). *Polymer Degradation and Stability*, *70*, 347.
Olsson, A. M., & Salmén, L. (2004). *Carbohydrate Research*, *339*, 813.
Ozawa, T. (1965). *Bulletin of the Chemical Society of Japan*, *88*, 6.
O'Sullivan, A. C. (1997). *Cellulose*, *4*, 173.
Proniewicz, L. M., Paluszkiewciz, C., Weselucha-Birczysimnska, A., Majcherczyk, H., Bara, S. A., & Konieczna, A. (2001). *Journal of Molecular Structure*, *596*, 163.
Quajai, S., & Shanks, R. A. (2005). *Polymer Degradation and Stability*, *89*, 327.

Satyanarayana, K. G., Ravikumar, K. K., Sukumaran, K., Mukherjee, P. S., Pillai, S. G. K., & Kulkarni, A. K. (1986). *Journal of Material Science*, *21*, 57.
Segal, L., Creely, A. E., Martin, A. E., & Conrad, C. M. (1959). *Textile Research Journal*, *29*, 786.
TAPPI. (2006). *Acid insoluble lignin in wood and pulp T 222 om-06*. US Technical Association of Pulp and Paper Industry.
TAPPI. (2012). *Ash in wood, pulp, paper and paperboard: Combustion at 525 °C T211 om-02*. US Technical Association of Pulp and Paper Industry.
Varhegyi, G., Antal, M. J., Szekely, T., Till, F., & Jakab, E. (1988). *Energy & Fuels*, *2*, 267.
Willium, P. T., & Besler, S. (1996). *Renewable Energy*, *7*, 233.
Yao, F., Wu, Q., Lei, Y., Guo, W., & Xu, Y. (2008). *Polymer Degradation and Stability*, *93*, 90.